

## Optimization of quantized charge pumping using full counting statistics

Elina Potanina, Kay Brandner, and Christian Flindt

*Department of Applied Physics, Aalto University, 00076 Aalto, Finland*



(Received 11 June 2018; revised manuscript received 5 January 2019; published 24 January 2019)

We optimize the operation of single-electron charge pumps using full counting statistics techniques. To this end, we evaluate the statistics of pumped charge on a wide range of driving frequencies using Floquet theory, focusing here on the current and the noise. For charge pumps controlled by one or two gate voltages, we demonstrate that our theoretical framework may lead to enhanced device performance. Specifically, by optimizing the driving parameters, we predict a significant increase in the frequencies for which a quantized current can be produced. For adiabatic two-parameter pumps, we exploit that the pumped charge and the noise can be expressed as surface integrals over Berry curvatures in parameter space. Our findings are important for the efforts to realize high-frequency charge pumping, and our predictions may be verified using current technology.

DOI: [10.1103/PhysRevB.99.035437](https://doi.org/10.1103/PhysRevB.99.035437)

### I. INTRODUCTION

Single-electron pumps are important for a wide range of quantum technologies, and they have been proposed as precise current sources for metrological purposes [1–3]. The central goal is to transfer single electrons between two leads via a nanoscale island as accurately and as fast as possible. The gate voltages of the island are modulated periodically in time with the aim to generate a current given by the electron charge times the frequency of the drive; see Fig. 1. Single-electron pumping has been demonstrated in several experimental architectures, and both the accuracy and the driving speed have been significantly increased during recent years [1–26].

To achieve reliable loading and unloading of single electrons, it is generally favorable to operate the pumps at low frequencies [27,28]. This regime can be elegantly described using adiabatic theories [29–35]. However, to produce an appreciable current, the driving should be fast while maintaining faultless single-electron control. Moreover, pumps operating with a single modulated gate voltage only deliver a quantized current well beyond the adiabatic regime [15–25]. Various techniques have been developed to improve the accuracy of such nonadiabatic pumps at the quantized-current plateau [36,37]. On the other hand, efficient tools to optimize the driving frequency are still lacking, as it is challenging to develop theories that extend beyond the adiabatic approximation. Instead, nonadiabatic pumps have mainly been investigated using numerical approaches [16,38–40].

In this work, we employ full counting statistics techniques to optimize the operation of single-electron charge pumps. We use Floquet theory to evaluate the current and the fluctuations of the pumped charge order-by-order in either the frequency or the period of the drive and thereby develop a systematic understanding of charge pumps beyond the adiabatic approximation. For single-parameter pumps, we optimize the driving frequency by minimizing the noise over the pumped charge (the Fano factor) at high frequencies. For adiabatic pumps, the full counting statistics can be expressed as a surface integral over a Berry curvature in parameter space [41–44], which

we use to optimize the driving protocol. Moreover, from the high-frequency expansion we can estimate the breakdown frequency for which a quantized current can no longer be generated. Although, we focus here on the average and noise of the pumped charge, our theoretical framework is versatile, and it can readily be adapted to other quantities such as the higher cumulants or even the large-deviation statistics of the current [45].

### II. QUANTIZED CHARGE PUMPING

The Floquet theory that we develop below is applicable to a large class of open quantum systems that exchange particles (or heat) with external reservoirs and whose dynamics can be described by a Markovian (generalized) master equation. To be specific, we consider here periodically driven single-electron pumps that ideally transfer one electron from a source

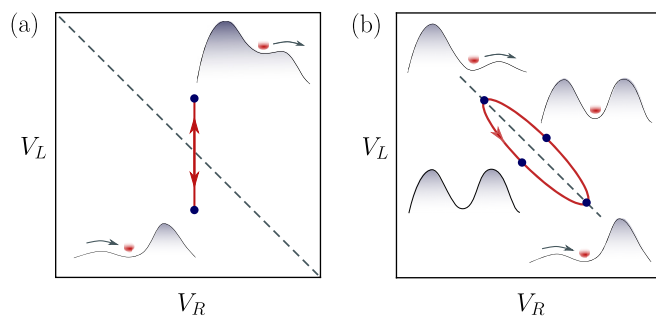


FIG. 1. Single-electron pumping. (a) Nonadiabatic charge pumping can be achieved by modulating a single gate voltage periodically in time as indicated by the red line. In this case, mainly the left barrier of the gate-defined potential is periodically modulated, as illustrated by the insets. The dashed line separates the stable charge configurations of the island (0 or 1 electrons). (b) Adiabatic pumping can be achieved by slowly modulating both gate voltages periodically in time as indicated by the positively oriented contour in red. The insets illustrate how both barriers are periodically modulated.

electrode to a collector in every single operation cycle. A charge pump consists of a nanoscale island whose dynamics is governed by the master equation

$$\frac{d}{dt}|P(t)\rangle = \mathbf{L}(t)|P(t)\rangle, \quad (1)$$

where the vector  $|P(t)\rangle = [p_0(t), p_1(t), p_2(t), \dots]^T$  contains the probabilities for the island to be occupied by 0, 1, 2, ... electrons. The rate matrix  $\mathbf{L}(t) = \mathbf{L}(t + \mathcal{T})$  describes the transitions between different charge states of the island, and  $\mathcal{T}$  is the period of the external drive. At all times, the product of the tunneling amplitudes to the source and the collector is kept so small that cotunneling processes can safely be ignored and we may consider sequential single-electron tunneling only.

To investigate the pumped current, we resolve the probability vector  $|P(t)\rangle = \sum_n |P(n, t)\rangle$  with respect to the number of electrons  $n$  that have been transferred during the time span  $[0, t]$  [46]. The charge-transfer statistics can then be expressed as  $P(n, t) = \langle 1|P(n, t)\rangle$  with all entries of the vector  $\langle 1|$  being 1. We also write the rate matrix as  $\mathbf{L}(t) = \mathbf{L}_0(t) + \mathbf{J}_+(t) + \mathbf{J}_-(t)$ , with  $\mathbf{J}_\pm(t)$  describing charge transfers to and from the collector [47]. The equations of motion,  $\frac{d}{dt}|P(n, t)\rangle = \mathbf{L}_0(t)|P(n, t)\rangle + \mathbf{J}_+(t)|P(n-1, t)\rangle + \mathbf{J}_-(t)|P(n+1, t)\rangle$ , are decoupled by introducing the counting field  $\chi$  via the definition  $|P(\chi, t)\rangle \equiv \sum_n |P(n, t)\rangle e^{in\chi}$ . We then arrive at a modified master equation for  $|P(\chi, t)\rangle$ ,

$$\frac{d}{dt}|P(\chi, t)\rangle = \mathbf{L}(\chi, t)|P(\chi, t)\rangle, \quad (2)$$

with  $\mathbf{L}(\chi, t) = \mathbf{L}(t) + (e^{i\chi} - 1)\mathbf{J}_+(t) + (e^{-i\chi} - 1)\mathbf{J}_-(t)$ . Formally, the solution  $|P(\chi, t)\rangle = \mathbf{U}(\chi, t)|P(\chi, 0)\rangle$  is given by the time-ordered exponential  $\mathbf{U}(\chi, t) = \hat{T}\{e^{\int_0^t dt' \mathbf{L}(\chi, t')}\}$  [48,49]. The moments of the pumped charge  $n$  then follow as  $\langle n^m \rangle(t) = \partial_{i\chi}^m \mathcal{M}(\chi, t)|_{\chi=0}$ , where  $\mathcal{M}(\chi, t) \equiv \sum_n P(n, t)e^{in\chi} = \langle 1|\mathbf{U}(\chi, t)|P(\chi, 0)\rangle$  is the moment generation function. Similarly, the cumulant generating function  $\mathcal{S}(\chi, t) \equiv \ln \mathcal{M}(\chi, t)$  delivers the cumulants as  $\langle\langle n^m \rangle\rangle(t) = \partial_{i\chi}^m \mathcal{S}(\chi, t)|_{\chi=0}$ . Below, we focus on the first two cumulants, namely the mean  $\langle\langle n \rangle\rangle = \langle n \rangle$  and the variance  $\langle\langle n^2 \rangle\rangle = \langle n^2 \rangle - \langle n \rangle^2$ , although higher cumulants can easily be obtained with little added effort.

### III. FLOQUET THEORY

We now make use of the periodicity of the drive. Building on the Floquet theorem [50], the time-evolution operator can be expressed as  $\mathbf{U}(\chi, t) = \sum_i e^{\lambda_i(\chi)t} |p_i(\chi, t)\rangle \langle p_i(\chi, 0)|$ , where  $|p_i(\chi, t)\rangle = |p_i(\chi, t + \mathcal{T})\rangle$  solves the Floquet eigenvalue problem<sup>1</sup>

$$\left[ \mathbf{L}(\chi, t) - \frac{d}{dt} \right] |p_i(\chi, t)\rangle = \lambda_i(\chi) |p_i(\chi, t)\rangle. \quad (3)$$

We then obtain  $\mathcal{S}(\chi, t) = \ln \sum_i e^{\lambda_i(\chi)t} \langle 1|p_i(\chi, t)\rangle$  and immediately see that the charge-transfer statistics after many

<sup>1</sup>We note that the left and right eigenvectors,  $\langle p_i(\chi, t)|$  and  $|p_i(\chi, t)\rangle$ , are not related by simple Hermitian conjugation, since the rate matrix  $\mathbf{L}(\chi, t)$  is not Hermitian.

periods  $\mathcal{N} \gg 1$  is fully encoded in the Floquet eigenvalue  $\phi(\chi) \equiv \max_i [\lambda_i(\chi)]$  with the largest real part

$$\mathcal{S}(\chi, \mathcal{N}\mathcal{T}) \simeq \mathcal{N}\mathcal{T}\phi(\chi). \quad (4)$$

Generally, however, it is a daunting task to determine  $\phi(\chi)$  and its dependence on the counting field. Nevertheless, as we go on to show, the eigenvalue can be found perturbatively in the frequency or the period of the drive.

### IV. ADIABATIC EXPANSION

We first evaluate the Floquet eigenvalue  $\phi(\chi)$  and the corresponding eigenvector, denoted as  $|p(\chi, t)\rangle$ , perturbatively in the driving frequency. In the adiabatic expansion, we treat the time derivative  $-\frac{d}{dt}$  in Eq. (3) as the perturbation [51]. Our adiabatic expansion can be formulated in terms of the instantaneous eigenvalue of  $\mathbf{L}(\chi, t)$  with the largest real part  $\lambda^{(0)}(\chi, t)$  and the corresponding eigenvectors  $\langle p^{(0)}(\chi, t)|$  and  $|p^{(0)}(\chi, t)\rangle$ . To begin with, we find from Eq. (3)

$$\phi(\chi) = \phi^{(0)}(\chi) - \int_0^{\mathcal{T}} \frac{dt}{\mathcal{T}} \langle p^{(0)}(\chi, t)| \frac{d}{dt} |p(\chi, t)\rangle, \quad (5)$$

where  $\phi^{(0)}(\chi) = \int_0^{\mathcal{T}} \frac{dt}{\mathcal{T}} \lambda^{(0)}(\chi, t)$  is the average of the instantaneous eigenvalue. Without a voltage bias, the contribution to the mean current from  $\phi^{(0)}(\chi)$  vanishes and the noise can be related to the conductance according to the fluctuation-dissipation theorem [52]. To proceed to higher orders, we expand the eigenvalue and eigenvector in the perturbation as  $\phi(\chi) = \sum_{k=0}^{\infty} \phi^{(k)}(\chi)$  and  $|p(\chi, t)\rangle = \sum_{k=0}^{\infty} |p^{(k)}(\chi, t)\rangle$  and collect terms of the same order in Eq. (5). To first order, we find  $\phi^{(1)}(\chi) = -\int_0^{\mathcal{T}} \frac{dt}{\mathcal{T}} \langle p^{(0)}(\chi, t)| \frac{d}{dt} |p^{(0)}(\chi, t)\rangle$  as previously established within a different framework [41–44]. For a device controlled by a single parameter, this term vanishes as we discuss below. To second order, we find

$$\phi^{(2)}(\chi) = -\int_0^{\mathcal{T}} \frac{dt}{\mathcal{T}} \langle p^{(0)}(\chi, t)| \frac{d}{dt} \mathbf{R}(\chi, t) \frac{d}{dt} |p^{(0)}(\chi, t)\rangle \quad (6)$$

having used  $|p^{(1)}(\chi, t)\rangle = \mathbf{R}(\chi, t) \frac{d}{dt} |p^{(0)}(\chi, t)\rangle$  as in standard perturbation theory, where  $\mathbf{R}(\chi, t)$  is the pseudoinverse of  $\mathbf{L}(\chi, t) - \lambda^{(0)}(\chi, t)$  [53]. Equation (6) is important as it allows us to evaluate the charge transfer statistics for single-parameter pumps to first nontrivial order in the driving frequency. Before demonstrating its usefulness with specific applications, we discuss our high-frequency expansion of the cumulant generating function.

### V. HIGH-FREQUENCY EXPANSION

The high-frequency expansion proceeds differently. Here, we write the time-evolution operator as  $\mathbf{U}(\chi, \mathcal{N}\mathcal{T}) = [\mathbf{U}(\chi, \mathcal{T})]^{\mathcal{N}} := e^{\mathcal{N}\mathcal{T}\mathbf{L}_F(\chi)}$  and identify the Floquet eigenvalue  $\phi(\chi)$  as the eigenvalue of  $\mathbf{L}_F(\chi)$  with the largest real part. Using a Floquet-Magnus expansion  $\mathbf{L}_F(\chi) = \sum_{k=0}^{\infty} \mathbb{L}^{(k)}(\chi)$ , we can then evaluate  $\phi(\chi)$  perturbatively in the period. The first two terms read  $\mathbb{L}^{(0)}(\chi) = \int_0^{\mathcal{T}} \frac{dt}{\mathcal{T}} \mathbf{L}(\chi, t)$  and  $\mathbb{L}^{(1)}(\chi) = \int_0^{\mathcal{T}} \frac{dt}{2} \int_0^{\mathcal{T}} \frac{dt'}{\mathcal{T}} [\mathbf{L}(\chi, t), \mathbf{L}(\chi, t')]$  [50,54,55]. In the high-frequency expansion  $\phi(\chi) = \sum_{k=0}^{\infty} \varphi^{(k)}(\chi)$ , the first term  $\varphi^{(0)}(\chi)$  is given by the eigenvalue of  $\mathbb{L}^{(0)}(\chi)$  with the

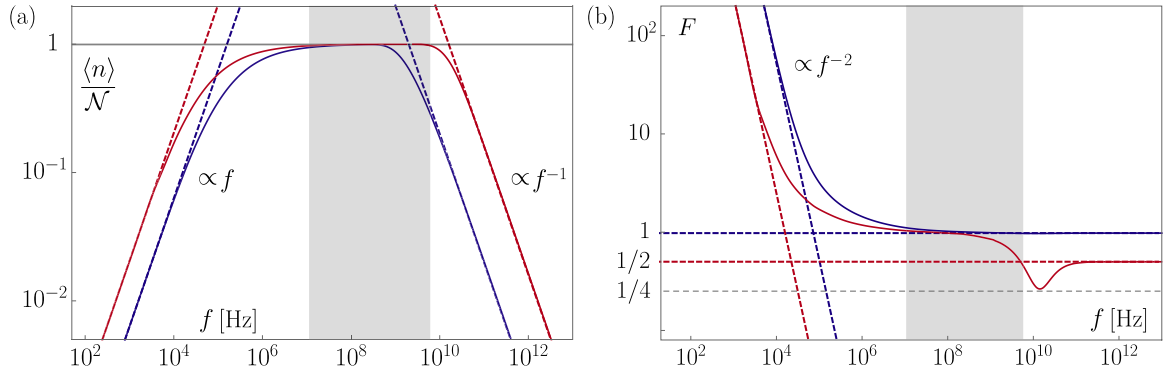


FIG. 2. Single-parameter pump. (a) Average pumped charge per period as a function of the driving frequency  $f$ . The solid lines are numerical results, while the dashed lines are the low- and high-frequency expansions. The red line is obtained with driving parameters that minimize the Fano factor at high frequencies. The shaded area indicates the quantized-current plateau for the optimized driving parameters. The system parameters are  $C = 10$  aF,  $G = 1.0 \times 10^{-4} \Omega^{-1}$ ,  $T = 0.2$  K, and  $\Gamma = G/4C = 2.5 \times 10^{12} \text{ s}^{-1}$ . The driving parameters are  $V_L^0 = 4$  mV (blue), 24 mV (red),  $V_R^0 = 0.8$  mV,  $V_s = 5 \mu\text{V}$ ,  $\mathcal{N}_g = 0.2$ . (b) The Fano factor  $F = \langle n^2 \rangle / \langle n \rangle$  of the pumped charge as a function of the driving frequency.

largest real part. Denoting the corresponding eigenvectors by  $|\mathbb{p}^{(0)}(\chi)\rangle$  and  $|\mathbb{p}^{(0)}(\chi)\rangle$ , the next term becomes  $\varphi^{(1)}(\chi) = \langle \mathbb{p}^{(0)}(\chi) | \mathbb{L}^{(1)}(\chi) | \mathbb{p}^{(0)}(\chi) \rangle$ . Thus, with the eigenvectors of  $\mathbb{L}^{(0)}(\chi)$  at hand, we can evaluate the charge-transfer statistics perturbatively in the period.

## VI. SINGLE-ELECTRON PUMP

We can now analyze a charge pump which is similar to those from recent experiments [2,7,10–13,15,17–20,22–25]. The pump consists of a metallic island operated in the Coulomb-blockade regime, where the island is either empty or occupied by one electron. The rate matrix then takes the simple form

$$\mathbf{L}(\chi, t) = \begin{pmatrix} -\Gamma_L^+(t) - \Gamma_R^+(t) & \Gamma_L^-(t) + \Gamma_R^-(t)e^{i\chi} \\ \Gamma_L^+(t) + \Gamma_R^+(t)e^{-i\chi} & -\Gamma_L^-(t) - \Gamma_R^-(t) \end{pmatrix},$$

where  $\Gamma_\alpha^\pm(t) = \frac{G_\alpha(t)}{q^2} \frac{\pm \Delta E(t)}{\exp[\pm \beta \Delta E(t)] - 1}$  is the rate at which tunneling occurs between the island and the leads, changing the occupation by  $\pm 1$  electron with charge  $-q$ . No voltage bias is applied, and  $\beta = 1/k_B T$  is the inverse temperature. The change of the electrostatic energy due to the addition of an electron reads  $\Delta E(t) = -E_c[\mathcal{N}_g + 2\{C_L V_L(t) + C_R V_R(t)\}/q]$ , where  $C_\alpha$  are the gate capacitances,  $E_c = q^2/2(C_L + C_R)$  is the charging energy, and the offset  $\mathcal{N}_g$  can be controlled with a backgate [3]. The barrier conductances depend exponentially on the gate voltages,  $G_\alpha(t) = G_\alpha \exp[V_\alpha(t)/V_s]$ , where  $V_s$  is known as the subthreshold slope [11].

## VII. SINGLE-PARAMETER PUMPING

We first consider a single-parameter pump, where the right gate voltage is kept constant,  $V_R(t) = -V_R^0$ , while the left one is subject to the harmonic drive,  $V_L(t) = -V_L^0[\cos(2\pi ft) + 1]$ . For low frequencies, the average of the pumped charge is obtained from Eq. (6). At low temperatures, where the tunneling rates  $\Gamma_L^-(t) \simeq \Gamma_R^+(t) \simeq 0$  are small, we

find

$$\frac{\langle n \rangle}{\mathcal{N}} \simeq f \int_0^1 ds \frac{[\Gamma_L^+(s)]^4 \left( \frac{d}{ds} [\Gamma_R^-(s)/\Gamma_L^+(s)] \right)^2}{[\Gamma_L^+(s) + \Gamma_R^-(s)]^5}, \quad (7)$$

having introduced the dimensionless time  $s = ft$  to show that the pumped charge is proportional to the driving frequency  $f$ . We also find that the variance can be expressed as  $\langle n^2 \rangle / \mathcal{N} = 2k_B T \int_0^1 ds G(s)/q^2 f$  in terms of the instantaneous linear conductance  $G(t)$  in accordance with the fluctuation-dissipation theorem. Combined with Eq. (7), we see that the Fano factor  $F = \langle n^2 \rangle / \langle n \rangle$  must be proportional to  $f^{-2}$  at low frequencies.

For high frequencies, we find the pumped charge from the first term in the Floquet-Magnus expansion,

$$\frac{\langle n \rangle}{\mathcal{N}} \simeq \frac{\Gamma}{f} \left[ \frac{q e^{V_R^0/V_s}}{2C(V_L^0 + V_R^0) - q\mathcal{N}_g} + \frac{q\sqrt{2\pi V_L^0/V_s}}{q\mathcal{N}_g - 2CV_R^0} \right]^{-1}. \quad (8)$$

Here, we have taken  $C_L = C_R = C$  and  $G_L = G_R = G$  with  $\Gamma = G/4C$  being an inverse  $RC$ -time. The gate voltage must change considerably compared to the subthreshold slope to open and close the left barrier, while being smaller than the charging energy, so that  $2CV_R^0 < q\mathcal{N}_g < 2C(V_L^0 + V_R^0)$ . The Fano factor thus becomes

$$F \simeq \frac{e^{-\frac{2V_R^0}{V_s}} [2C(V_L^0 + V_R^0) - q\mathcal{N}_g]^2 + \frac{V_s}{2\pi V_L^0} (q\mathcal{N}_g - 2CV_R^0)^2}{\left( e^{-\frac{V_R^0}{V_s}} [2C(V_L^0 + V_R^0) - q\mathcal{N}_g] + \sqrt{\frac{V_s}{2\pi V_L^0}} (q\mathcal{N}_g - 2CV_R^0) \right)^2}. \quad (9)$$

Figure 2 shows numerical results for the pumped charge and the Fano factor together with our approximations. The blue curves illustrate the good agreement between the numerics and our perturbative results. With Eqs. (7) and (8) we quantitatively explain the low- and high-frequency dependence of the pumped charge, which previously has been observed in numerical calculations [16]. Moreover, our results allow us to optimize the driving parameters. By inspecting Eq. (9), we see that the Fano factor takes

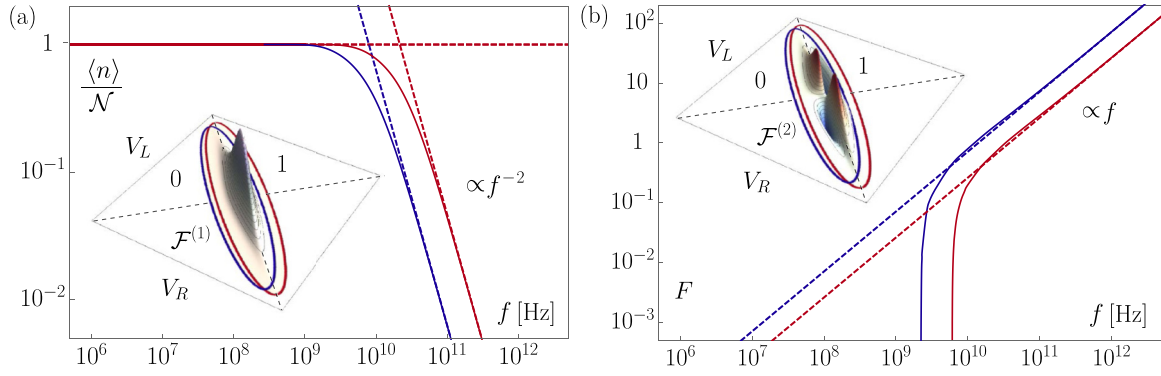


FIG. 3. Pumped charge (a) and the Fano factor (b) for the two-parameter pump. The driving protocol  $\mathbf{V}(t) = -V^0[\cos(2\pi ft) + \alpha, \cos(2\pi ft + \vartheta) + \alpha]^T$  is shown together with the Berry curvatures  $\mathcal{F}^{(j)}$  in the insets, where the stable charge configuration of the island is also indicated (0 or 1 electrons). The solid lines are numerical results, while the dashed lines are the low- and high-frequency approximations. The system parameters are given in Fig. 2. The driving parameters are  $V^0 = 8$  mV,  $\vartheta = 1.02\pi$ ,  $\mathcal{N}_g = 2$ , and  $\alpha = 1.01$  (blue),  $\alpha = \mathcal{N}_g/2 = 1$  (red).

the minimal value of  $1/2$  if  $e^{-\frac{V_R^0}{V_s}} [2C(V_L^0 + V_R^0) - q\mathcal{N}_g] = \sqrt{\frac{V_s}{2\pi V_L^0}} (q\mathcal{N}_g - 2CV_R^0)$ . We then obtain an optimal ratio of the noise over the pumped charge, which simplifies to  $\langle n \rangle / \mathcal{N} \simeq (\Gamma/2f)\sqrt{V_s/2\pi V_L^0}(\mathcal{N}_g - 2CV_R^0/q)$ . The red lines in Fig. 2 show the results of this optimization. Importantly, compared to the generic blue curve, we obtain an order-of-magnitude increase in the frequencies, for which a quantized current can be produced. Interestingly, the Fano factor dips below  $1/2$  at the end of the quantized-current plateau and almost reaches  $1/4$ , signaling a transition to a new transport regime.

### VIII. TWO-PARAMETER PUMPING

Next, we modulate both voltages periodically in time,  $\mathbf{V}(t) = [V_L(t), V_R(t)]^T$ . In the adiabatic regime, we can then write  $\phi^{(1)}(\chi) = \pm f \iint_{\mathcal{S}} dV_L dV_R \mathcal{F}(\chi, \mathbf{V})$  by virtue of Stokes' theorem. Here, the sign is given by the orientation of the contour enclosing the surface  $\mathcal{S}$  in the parameter space, and  $\mathcal{F}(\chi, \mathbf{V}) = [-\partial_{V_L}, \partial_{V_R}] \cdot \langle p^{(0)}(\chi, \mathbf{V}) | \nabla_{\mathbf{V}} | p^{(0)}(\chi, \mathbf{V}) \rangle$  is a classical analog of the Berry curvature in quantum mechanics [41–44]. Clearly, if only one voltage is varied, the surface area vanishes, and  $\phi^{(1)}(\chi) = 0$ . For the pumped charge [56,57], we find  $\langle n \rangle / \mathcal{N} \simeq \pm \iint_{\mathcal{S}} dV_L dV_R \mathcal{F}^{(1)}(\mathbf{V})$  with  $\mathcal{F}^{(m)}(\mathbf{V}) = \partial_{i\chi}^m \mathcal{F}(\chi, \mathbf{V})|_{\chi=0}$  and

$$\mathcal{F}^{(1)} = \frac{q\beta e^{(V_L+V_R)/V_s}}{4V_s(e^{V_L/V_s} + e^{V_R/V_s})^2 \cosh^2(\beta\Delta E/2)} \quad (10)$$

as shown in Fig. 3(a). For the variance  $\langle \langle n^2 \rangle \rangle / \mathcal{N} \simeq 2k_B T \int_0^1 ds G(s)/q^2 f \pm \iint_{\mathcal{S}} dV_L dV_R \mathcal{F}^{(2)}(\mathbf{V})$ , we have

$$\mathcal{F}^{(2)} = \frac{q\beta e^{(V_R+V_L)/V_s} (e^{V_R/V_s} - e^{V_L/V_s}) \sinh^4(\beta\Delta E/2)}{32V_s(e^{V_R/V_s} + e^{V_L/V_s})^3 \sinh^3(\beta\Delta E)} \quad (11)$$

as shown in Fig. 3(b). We can now position our contour so that the pumped charge is maximized and the

noise is minimized. To this end, we exploit the symmetry  $\mathcal{F}^{(j)}(V_L, V_R) = \mathcal{F}^{(j)}(-V_C - V_L, -V_C - V_R)$ ,  $j = 1, 2$ , about the point  $(-V_C/2, -V_C/2)$  with  $V_C = q/2C$ , together with the symmetry  $\mathcal{F}^{(j)}(V_L, V_R) = (-1)^{j-1} \mathcal{F}^{(j)}(V_R, V_L)$  across the line  $V_L = V_R$ . Specifically, for a fixed shape of the contour, the contribution to the variance vanishes if the contour is placed symmetrically across the line  $V_L = V_R$ . In that case, the noise is due to equilibrium fluctuations only. Moreover, the pumped charge is maximized if the contour is also symmetric about the point  $(-V_C/2, -V_C/2)$ .

Figure 3 shows the pumped charge and the Fano factor for the driving protocols indicated in the insets together with the Berry curvatures. As in the experiments of Refs. [7,11], we consider elliptical contours in parameter space. Both the red and the blue ellipse minimize the noise, while only the red one also maximizes the pumped charge. In the high-frequency regime, the pumped charge  $\langle n \rangle / \mathcal{N} \simeq \mathcal{T} \partial_{i\chi} \phi^{(1)}(\chi)|_{\chi=0}$  decreases as  $1/f^2$ , since there is no contribution from  $\phi^{(0)}(\chi)$  without a voltage bias. The variance, by contrast, is dominated by thermal fluctuations described by  $\phi^{(0)}(\chi)$ . We then have  $\langle \langle n^2 \rangle \rangle / \mathcal{N} \simeq \mathcal{T} \partial_{i\chi}^2 \phi^{(0)}(\chi)|_{\chi=0}$ , implying that the Fano factor is proportional to the frequency. These conclusions are supported by our numerical results in Fig. 3. At low frequencies, the Fano factor is very small (not visible in the figure) and inversely proportional to the frequency. Importantly, from our high-frequency expansion, we get a good estimate of the breakdown frequency for which a quantized current can no longer be generated.

### IX. CONCLUSIONS

We have employed full counting statistics techniques to optimize the operation of charge pumps. To this end, we have used Floquet theory to evaluate the cumulant generating function for the distribution of pumped charge perturbatively in the frequency or the period of the drive. For the device optimization, we have focused on the average and the variance (noise) of the pumped charge, but higher cumulants, or even the large-deviation statistics, can be obtained along the same lines with little added effort. Our theoretical framework covers

a wide range of driving frequencies, in the adiabatic regime and for fast driving, and it is useful for practical device optimization. The advances reported here were made possible due to the progress made in theories of driven systems. Our work demonstrates that full counting statistics is a powerful tool to optimize charge pumps, and our predictions may be confirmed in future experiments.

## ACKNOWLEDGMENTS

We thank V. Kashcheyevs and T. Ojanen for useful discussions. K.B. acknowledges support from Academy of Finland (Contract No. 296073). The work was supported by Academy of Finland (Projects No. 308515 and No. 312299). All authors are associated with the Centre for Quantum Engineering at Aalto University.

- 
- [1] A. A. Odintsov, Single electron transport in a two-dimensional electron gas system with modulated barriers: A possible dc current standard, *Appl. Phys. Lett.* **58**, 2695 (1991).
- [2] S. P. Giblin, M. Kataoka, J. D. Fletcher, P. See, T. J. B. M. Janssen, J. P. Griffiths, G. A. C. Jones, I. Farrer, and D. A. Ritchie, Towards a quantum representation of the ampere using single electron pumps, *Nat. Commun.* **3**, 930 (2012).
- [3] J. P. Pekola, O.-P. Saira, V. F. Maisi, A. Kemppinen, M. Möttönen, Yu. A. Pashkin, and D. V. Averin, Single-electron current sources: Toward a refined definition of the ampere, *Rev. Mod. Phys.* **85**, 1421 (2013).
- [4] L. P. Kouwenhoven, A. T. Johnson, N. C. van der Vaart, C. J. P. M. Harmans, and C. T. Foxon, Quantized Current in a Quantum-Dot Turnstile Using Oscillating Tunnel Barriers, *Phys. Rev. Lett.* **67**, 1626 (1991).
- [5] H. Pothier, P. Lafarge, C. Urbina, D. Esteve, and M. H. Devoret, Single-electron pump based on charging effects, *Europhys. Lett.* **17**, 249 (1992).
- [6] M. W. Keller, J. M. Martinis, N. M. Zimmerman, and A. H. Steinbach, Accuracy of electron counting using a 7-junction electron pump, *Appl. Phys. Lett.* **69**, 1804 (1996).
- [7] Y. Ono and Y. Takahashi, Electron pump by a combined single-electron/field-effect-transistor structure, *Appl. Phys. Lett.* **82**, 1221 (2003).
- [8] A. M. Robinson and V. I. Talyanskii, Shot Noise in the Current of a Surface Acoustic-Wave-Driven Single-Electron Pump, *Phys. Rev. Lett.* **95**, 247202 (2005).
- [9] J. P. Pekola, J. J. Vartiainen, M. Möttönen, O.-P. Saira, M. Meschke, and D. V. Averin, Hybrid single-electron transistor as a source of quantized electric current, *Nat. Phys.* **4**, 120 (2007).
- [10] A. Fujiwara, K. Nishiguchi, and Y. Ono, Nanoampere charge pump by single-electron ratchet using silicon nanowire metal-oxide-semiconductor field-effect transistor, *Appl. Phys. Lett.* **92**, 042102 (2008).
- [11] X. Jehl, B. Voisin, T. Charron, P. Clapera, S. Ray, B. Roche, M. Sanquer, S. Djordjevic, L. Devoille, R. Wacquez, and M. Vinet, Hybrid Metal-Semiconductor Electron Pump for Quantum Metrology, *Phys. Rev. X* **3**, 021012 (2013).
- [12] G. Yamahata, K. Nishiguchi, and A. Fujiwara, Gigahertz single-trap electron pumps in silicon, *Nat. Commun.* **5**, 5038 (2014).
- [13] A. Rossi, T. Tantt, K. Y. Tan, I. Iisakka, R. Zhao, K. W. Chan, G. C. Tettamanzi, S. Rogge, A. S. Dzurak, and M. Möttönen, An accurate single-electron pump based on a highly tunable silicon quantum dot, *Nano Lett.* **14**, 3405 (2014).
- [14] M. R. Connolly, K. L. Chiu, S. P. Giblin, M. Kataoka, J. D. Fletcher, C. Chua, J. P. Griffiths, G. A. C. Jones, V. I. Fal'ko, C. G. Smith, and T. J. B. M. Janssen, Gigahertz quantized charge pumping in graphene quantum dots, *Nat. Nanotech.* **8**, 417 (2013).
- [15] M. D. Blumenthal, B. Kaestner, L. Li, S. Giblin, T. J. B. M. Janssen, M. Pepper, D. Anderson, G. Jones, and D. A. Ritchie, Gigahertz quantized charge pumping, *Nat. Phys.* **3**, 343 (2007).
- [16] B. Kaestner, V. Kashcheyevs, S. Amakawa, M. D. Blumenthal, L. Li, T. J. B. M. Janssen, G. Hein, K. Pierz, T. Weimann, U. Siegner, and H. W. Schumacher, Single-parameter nonadiabatic quantized charge pumping, *Phys. Rev. B* **77**, 153301 (2008).
- [17] S. P. Giblin, S. J. Wright, J. D. Fletcher, M. Kataoka, M. Pepper, T. J. B. M. Janssen, D. A. Ritchie, C. A. Nicoll, D. Anderson, and G. A. C. Jones, An accurate high-speed single-electron quantum dot pump, *New J. Phys.* **12**, 073013 (2010).
- [18] M. Kataoka, J. D. Fletcher, P. See, S. P. Giblin, T. J. B. M. Janssen, J. P. Griffiths, G. A. C. Jones, I. Farrer, and D. A. Ritchie, Tunable Nonadiabatic Excitation in a Single-Electron Quantum Dot, *Phys. Rev. Lett.* **106**, 126801 (2011).
- [19] L. Fricke, M. Wulf, B. Kaestner, F. Hohls, P. Mirovsky, B. Mackrodt, R. Dolata, T. Weimann, K. Pierz, U. Siegner, and H. W. Schumacher, Self-Referenced Single-Electron Quantized Current Source, *Phys. Rev. Lett.* **112**, 226803 (2014).
- [20] N. Ubbelohde, F. Hohls, V. Kashcheyevs, T. Wagner, L. Fricke, B. Kästner, K. Pierz, H. W. Schumacher, and R. J. Haug, Partitioning of on-demand electron pairs, *Nat. Nanotech.* **10**, 46 (2015).
- [21] B. Kaestner and V. Kashcheyevs, Non-adiabatic quantized charge pumping with tunable-barrier quantum dots: A review of current progress, *Rep. Prog. Phys.* **78**, 103901 (2015).
- [22] F. Stein, D. Drung, L. Fricke, H. Scherer, F. Hohls, C. Leicht, M. Götz, C. Krause, R. Behr, E. Pesel, K. Pierz, U. Siegner, F. J. Ahlers, and H. W. Schumacher, Validation of a quantized-current source with 0.2 ppm uncertainty, *Appl. Phys. Lett.* **107**, 103501 (2015).
- [23] G. Yamahata, S. P. Giblin, M. Kataoka, T. Karasawa, and A. Fujiwara, Gigahertz single-electron pumping in silicon with an accuracy better than 9.2 parts in  $10^7$ , *Appl. Phys. Lett.* **109**, 013101 (2016).
- [24] Y.-H. Ahn, C. Hong, Y. Ghee, Y. Chung, Y.-P. Hong, M.-H. Bae, and N. Kim, Upper frequency limit depending on potential shape in a QD-based single electron pump, *J. Appl. Phys.* **122**, 194502 (2017).
- [25] R. Zhao, A. Rossi, S. P. Giblin, J. D. Fletcher, F. E. Hudson, M. Möttönen, M. Kataoka, and A. S. Dzurak, Thermal-error regime in high-accuracy gigahertz single-electron pumping, *Phys. Rev. Appl.* **8**, 044021 (2017).
- [26] J. Brun-Picard, S. Djordjevic, D. Leprat, F. Schopfer, and W. Poirier, Practical Quantum Realization of the Ampere from the Elementary Charge, *Phys. Rev. X* **6**, 041051 (2016).
- [27] M. Moskalets and M. Büttiker, Floquet scattering theory of quantum pumps, *Phys. Rev. B* **66**, 205320 (2002).

- [28] M. Moskalets and M. Büttiker, Dissipation and noise in adiabatic quantum pumps, *Phys. Rev. B* **66**, 035306 (2002).
- [29] P. W. Brouwer, Scattering approach to parametric pumping, *Phys. Rev. B* **58**, 10135(R) (1998).
- [30] I. L. Aleiner and A. V. Andreev, Adiabatic Charge Pumping in Almost Open Dots, *Phys. Rev. Lett.* **81**, 1286 (1998).
- [31] T. A. Shutenko, I. L. Aleiner, and B. L. Altshuler, Mesoscopic fluctuations of adiabatic charge pumping in quantum dots, *Phys. Rev. B* **61**, 10366 (2000).
- [32] J. E. Avron, A. Elgart, G. M. Graf, and L. Sadun, Geometry, statistics, and asymptotics of quantum pumps, *Phys. Rev. B* **62**, R10618 (2000).
- [33] Yu. Makhlin and A. D. Mirlin, Counting Statistics for Arbitrary Cycles in Quantum Pumps, *Phys. Rev. Lett.* **87**, 276803 (2001).
- [34] O. Entin-Wohlman, A. Aharony, and Y. Levinson, Adiabatic transport in nanostructures, *Phys. Rev. B* **65**, 195411 (2002).
- [35] J. Splettstoesser, M. Governale, J. König, and R. Fazio, Adiabatic Pumping Through Interacting Quantum Dots, *Phys. Rev. Lett.* **95**, 246803 (2005).
- [36] V. Kashcheyevs and B. Kaestner, Universal Decay Cascade Model for Dynamic Quantum Dot Initialization, *Phys. Rev. Lett.* **104**, 186805 (2010).
- [37] V. Kashcheyevs and J. Timoshenko, Quantum Fluctuations and Coherence in High-Precision Single-Electron Capture, *Phys. Rev. Lett.* **109**, 216801 (2012).
- [38] J. Ohkubo and T. Egge, A direct numerical method for obtaining the counting statistics for stochastic processes, *J. Stat. Mech.* (2010) P06013.
- [39] A. Croy and U. Saalmann, Nonadiabatic rectification and current reversal in electron pumps, *Phys. Rev. B* **86**, 035330 (2012).
- [40] A. Croy and U. Saalmann, Full counting statistics of a nonadiabatic electron pump, *Phys. Rev. B* **93**, 165428 (2016).
- [41] N. A. Sinitsyn and I. Nemenman, The Berry phase and the pump flux in stochastic chemical kinetics, *Europhys. Lett.* **77**, 58001 (2007).
- [42] N. A. Sinitsyn and I. Nemenman, Universal Geometric Theory of Mesoscopic Stochastic Pumps and Reversible Ratchets, *Phys. Rev. Lett.* **99**, 220408 (2007).
- [43] J. Ren, P. Hänggi, and B. Li, Berry-Phase-Induced Heat Pumping and its Impact on the Fluctuation Theorem, *Phys. Rev. Lett.* **104**, 170601 (2010).
- [44] H. P. Goswami, B. K. Agarwalla, and U. Harbola, Geometric effects in nonequilibrium electron transfer statistics in adiabatically driven quantum junctions, *Phys. Rev. B* **93**, 195441 (2016).
- [45] H. Touchette, The large deviation approach to statistical mechanics, *Phys. Rep.* **478**, 1 (2009).
- [46] M. B. Plenio and P. L. Knight, The quantum-jump approach to dissipative dynamics in quantum optics, *Rev. Mod. Phys.* **70**, 101 (1998).
- [47] M. Benito, M. Niklas, and S. Kohler, Full-counting statistics of time-dependent conductors, *Phys. Rev. B* **94**, 195433 (2016).
- [48] F. Pistolesi, Full counting statistics of a charge shuttle, *Phys. Rev. B* **69**, 245409 (2004).
- [49] E. Potanina and C. Flindt, Electron waiting times of a periodically driven single-electron turnstile, *Phys. Rev. B* **96**, 045420 (2017).
- [50] M. Bukov, L. D'Alessio, and A. Polkovnikov, Universal high-frequency behavior of periodically driven systems: from dynamical stabilization to Floquet engineering, *Adv. Phys.* **64**, 139 (2015).
- [51] V. Cavina, A. Mari, and V. Giovannetti, Slow Dynamics and Thermodynamics of Open Quantum Systems, *Phys. Rev. Lett.* **119**, 050601 (2017).
- [52] Ya. M. Blanter and M. Büttiker, Shot noise in mesoscopic conductors, *Phys. Rep.* **336**, 1 (2000).
- [53] C. Flindt, T. Novotný, A. Braggio, and A.-P. Jauho, Counting statistics of transport through Coulomb blockade nanostructures: High-order cumulants and non-Markovian effects, *Phys. Rev. B* **82**, 155407 (2010).
- [54] S. Blanes, F. Casas, J. A. Oteo, and J. Ros, The Magnus expansion and some of its applications, *Phys. Rep.* **470**, 151 (2009).
- [55] T. Kuwahara, T. Mori, and K. Saito, Floquet-Magnus theory and generic transient dynamics in periodically driven many-body quantum systems, *Ann. Phys.* **367**, 96 (2016).
- [56] J. P. Pekola, J. J. Toppari, M. Aunola, M. T. Savolainen, and D. V. Averin, Adiabatic transport of Cooper pairs in arrays of Josephson junctions, *Phys. Rev. B* **60**, 9931(R) (1999).
- [57] Y. Levinson, O. Entin-Wohlman, and P. Wölfle, Pumping at resonant transmission and transferred charge quantization, *Physica A* **302**, 335 (2001).